Contrib Mineral Petrol (1985) 90:36–44

Contributions to Mineralogy and Petrology

Experimental determination of cation diffusivities in aluminosilicate garnets

I. Experimental methods and interdiffusion data

Stephen C. Elphick*, Jibamitra Ganguly and Timothy P. Loomis
Department of Geosciences, University of Arizona, Tucson, AZ 85721

Abstract. We have carried out diffusion couple experiments using pairs of single crystals of natural garnet of dissimilar compositions in the range of 30–40 Kbar, 1,300–1,500° C, and measured the induced diffusion profiles by microprobe scanning across the interface. Significant modifications to, and experimentation with, the design of the pressure cell, furnace assembly and sample geometry were needed to obtain measurable volume diffusion at controlled $P-T$ conditions.

The diffusion profiles in the pyrope-almandine couples are short enough that retrieval of diffusion data from them must await deconvolution analysis to resolve the effect of spatial averaging of the microprobe beam. However, the profiles in the spessartine-almandine couples are sufficiently long to obviate convolution analysis. They yield interdiffusion coefficients (D) at 40 Kbar of

$$D=0.82\times10^{-5}\exp(-53.6\pm4.9\ \text{Kcal/RT})\ \text{cm}^2/\text{s}$$

and

$$D=1.2\times10^{-5}\exp(-57.1\pm8.4\ \text{Kcal/RT})\ \text{cm}^2/\text{s}$$

for Fe-rich and Mn-rich compositions, respectively, and an activation volume of $\sim4.7\ \text{cm}^3$/mole. Preliminary analysis of profiles in a pyrope-almandine couple at ~40 Kbar, 1,440° C suggests Fe-Mg interdiffusion to be an order of magnitude slower that Fe-Mn interdiffusion, and to increase with Fe/Mg ratio. The interdiffusion data reported here are in sharp disagreement with those of Freer (1979) and Duckworth and Freer (in Freer 1981) on Fe-Mn and Fe-Mg interdiffusion, respectively.

Introduction

Garnet is one of the most important minerals in crustal and mantle metamorphic rocks used to interpret geological processes. Compositional zoning is being used increasingly as a means of interpreting the history of rocks. The usefulness of compositional zoning derives from (1) the sensitivity of garnet composition to the mineral assemblage and to temperature, pressure, and other conditions of formation and (2) small diffusion rates that enable garnet to retain evidence of its growth and reaction history. Garnet is an ideal recorder of past conditions because it is physically resistant, it is abundant in many bulk compositions and the composition of aluminous garnets can be easily measured with the microprobe.

Diffusion is an important process in garnet that controls the usefulness of compositional zoning. First, diffusion tends to eliminate zoning generated by fractionation processes during the growth of low-grade garnets. Fortunately, diffusion seems to be slow enough in garnets to preserve growth-induced zoning until moderate grades of metamorphism in regional rocks (Loomis 1983). However, the influence of diffusion on growth zoning probably becomes significant at staurolite grade. At higher grades, the rate of diffusion is appropriate for inducing diffusion zoning profiles on the edges of crystals but not so effective that it homogenizes the crystals. When diffusion in garnet is important, it can be modeled because diffusion within garnet is isotropic owing to its isometric symmetry.

The application of diffusion analysis to compositional zoning in garnet can be resolved approximately into two studies. These two major fields of zoning studies are discussed in the overview of the subject by Loomis (1983). Growth zoning in garnet usually results in conspicuous complementary zoning profiles of Mn and Fe, with only small change in the concentration of the pyrope component, which is present in small concentration. Relaxation of the growth-induced zoning involves principally Fe-Mn exchange. On the other hand, the high-grade exchange that causes edge zoning in garnets affects principally Mg and Fe; the concentration of Mn in the high-grade garnets is small because it is distributed in the usually abundant garnet present. For convenience, we will separate application of results into the corresponding problems of (1) Mn-Fe exchange in Mg- and Ca-poor garnets and (2) Mg-Fe exchange in Mn- and Ca-poor garnets.

Three major problems dealing with diffusion in garnet are (1) the difficulty of measuring very small diffusion coefficients within the laboratory time scale, (2) the multicomponent character of exchange in a mineral with 4 components, and (3) the probable compositional dependence of diffusion coefficients. In this paper we describe the experimental techniques used to obtain data on interdiffusion in garnets at high temperatures, and present the results on interdiffusion coefficients that are accurate enough to pro-

* *Present address:* Grant Institute of Geology, University of Edinburgh, Edinburgh EH9 3JW, Great Britain

Offprint requests to: J. Ganguly

pose diffusion models for the two practical problems addressed above. In the second paper (Loomis et al. 1985), we investigate the multicomponent interactions and compositional dependencies that can be measured in our data, primarily on Fe-Mn interdiffusion, by matching multicomponent, compositionally-dependent simulations to the data. For reasons discussed later in this paper, detailed modeling of Fe-Mg diffusion data will be presented in a separate paper.

Experimental methods

We discuss below selected aspects of our experimental methods, including design developments, which convey an idea of the problems attending this experimental project, and the precision in our knowledge of the diffusion parameters retrieved from the experimental data.

Diffusion couples and experimental conditions

Early attempts by us to obtain Fe-Mg diffusion data in garnet by using diffusion couples consisting of a cylindrical block of Mg-rich garnet single crystal along with sintered powders of either olivine or clinopyroxene or almandine of dissimilar Fe/Mg ratio were unsuccessful. The garnet-olivine/clinopyroxene couples revealed interface chemical breakdown even though the experimental P−T conditions were well within the garnet stability field according to the experimental data of Perkins (1983), whereas the pyrope-almandine-powder couple showed virtually no measurable diffusion. We believe that the failure of the last couple is due to the preferential channeling of diffusion along tortuous grain boundaries, as the run duration (48 h at 1,400° C) was adequate, as will be shown later, to produce a significantly larger volume diffusion profile. Consequently, the use of sintered powder may, in general, be a questionable technique in the study of volume diffusion process (also see Buening and Buseck 1973). We, therefore, decided to use garnet-garnet couples made of two single crystals of garnets of dissimilar composition with a highly polished interface. Zoning profiles induced in such couples were, in principle, also capable of yielding more information on the compositional dependencies of diffusion coefficients. Some exploratory experiments were conducted with powdered mixtures of these garnets to decide on $P-T$ conditions at which the diffusion experiments could be carried out without risking their chemical decomposition.

Since diffusion in garnet is very slow, relatively high temperatures are required to induce experimentally an adequate zoning profile, which could be measured with the spatial resolution of a microprobe, and modeled to retrieve cation diffusivities. This, in turn, required very high pressures to ensure stability of garnets, especially at Mg-rich compositions. All experiments were, therefore, carried out at pressures of ~35–40 Kbar in a piston-cylinder apparatus using solid pressure media with a graphite internal resistance furnace, and a pressure vessel with a 1/2 inch I.D. carbide core and carbide piston. The experimental temperature range was 1300 to 1,475° C. The diffusion in garnet was found to be very sluggish so that it was impractical at this stage to attempt experiments at lower temperatures.

At such high pressures, we found it very difficult to preserve the mechanical integrity of the garnet-garnet couple of cylindrical geometry over sufficiently large domains

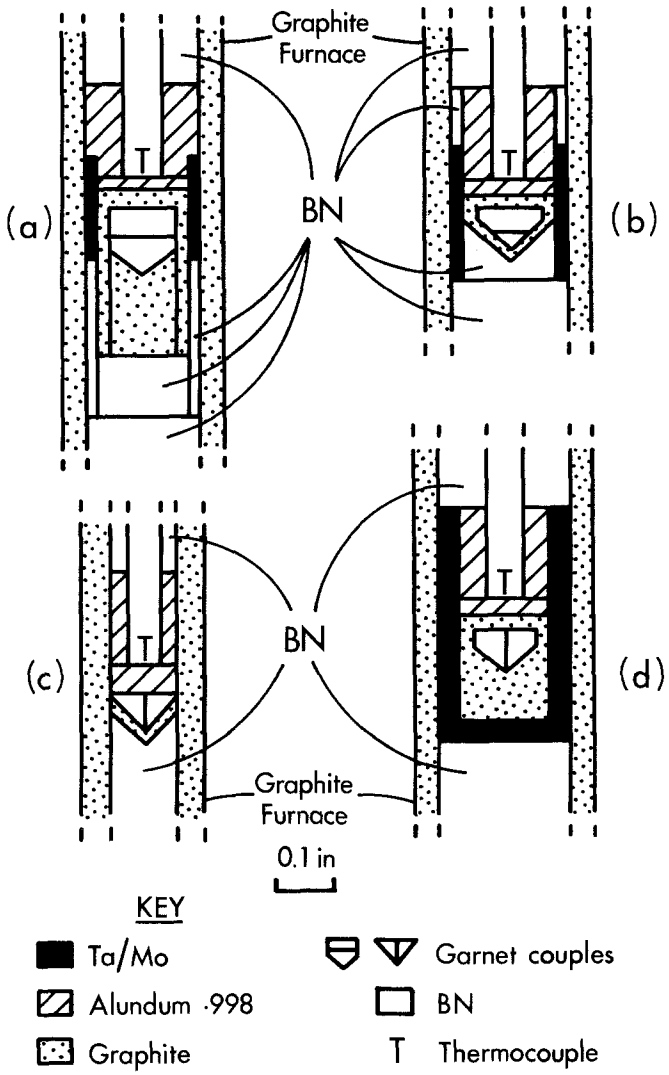

Fig. 1. Geometries of the garnet-garnet diffusion couple and adjacent section of pressure cell used successfully in the high $P-T$ experiments in the Piston-Cylinder apparatus. Spessartine-almandine couples did not seal unless the interface was vertical (see text)

to ensure volume diffusion. In similar experiments with olivine, Misener (1974) did not seem to have experienced a similar problem of mechanical failure. The mechanical failures were primarily due to (1) the relatively brittle behavior of garnet, (2) large uniaxial stress in the solid pressure medium, especially during compression at room temperature when stress redistribution by flow is minimal, and (3) high local stress at the contact of a garnet wafer and the thermocouple junction. The last problem is due to the extreme rigidity of the alumina ceramic (99.8% Al_2O_3) in which the thermocouple had to be encased to preserve its mechanical and chemical stability. The designs of sample geometry and pressure cell that proved to be most successful in preserving the mechanical integrity of the interface are illustrated in Fig. 1, and a picture of a section of a "successful" pyrope-almandine couple is shown in Fig. 2.

The principal features of the design are (1) a 90° cone at the bottom of the diffusion-couple, which helped redistribution of uniaxial stress, (2) a thin (0.025 inch) washer, machined from high purity synthetic corundum, between the thermocouple tip and the diffusion couple, which spread

Fig. 2. An example of a "successful" pyrope-almandine couple, which preserved the (horizontal) interface after a run at 38 Kbar, 1,475° C, 26.7 h (Run # 16). Athough the garnets were partly fractured, most of the interface was preserved intact. The interface is indicated by horizontal lines on the sides of the couple. The sectional width of the couple is 0.25 cm

the point-load against the hard thermocouple ceramic, and (3) a 0.025 inch thick graphite disk above the garnet, that acted as a cushion between the garnet and the alumina disk.

Individual garnets were prepared by polishing down to a final grit size of 1/4 micron the largest possible slices of gem quality material. Circular cores were then cut from the central flat areas of the polished slices, which were optically scratch-free and clean, and the couples constructed by gluing the requisite polished faces together. The resultant pair was then glued onto a glass rod, and lathed along with the rod to final size and shape using diamond tools. After shaping, the couples were unglued from the mounting rods, separated, and thoroughly cleaned before final assembly in a graphite capsule. This capsule was inserted into the 1/2 inch furnace-pressure cell assembly, as shown in Fig. 1.

It will be noticed in Fig. 1 that we have used couples with both horizontal and vertical interfaces. The couples with horizontal interfaces are preferable, as there is virtually no temperature gradient along the interface, and the entire interface is located close to the thermocouple junction. The horizontal interface was used successfully in the pyrope-almandine diffusion couples, but for the almandine-spessartine couples, it invariably parted after the samples were unloaded from the pressure cells. We usually found several horizontal partings through the pressure cell, including the diffusion couple, owing to extension during unloading. For the pyrope-almandine couple, it was possible to reduce the tension fractures by very slow decompression, but this technique failed to hold together the almandine-spessartine interface, even with decompression under relatively hot condition. Consequently, we had to use the vertical interface for the almandine-spessartine couple. This technique worked very well in preserving the cohesion of the interface, but introduced the additional problem of potentially larger uncertainty in the measurement of temperature of the induced diffusion profile. The reason for the superior cohesiveness of the horizontal interface of the pyrope-almandine couple relative to that of the almandine-spessartine couple is not clear, but probably lies in the smaller volume disparity of the pyrope and almandine compositions (molar volume difference = 0.494 cm^3 or 0.004%) compared to that of the almandine and spessartine compositions (molar volume difference = 3.134 cm^3 or 0.027%).

Temperature gradient and the furnace-pressure cell assembly

Because of the combined thicknesses of ceramic, graphite, and garnet, the final geometry placed the thermocouple junction 0.1″ from the interface of interest. This raised the problem of whether the recorded and interface temperatures were identical because in this type of pressure cell-furnace assembly, there could be a considerable temperature gradient over a vertical distance of 0.1″ (Cohen et al. 1967; Kushiro 1975). To eliminate thermal gradients, the center of the full furnace length was located midway between thermocouple junction and interface, on the usual assumption that the furnace hotspot lay at its central section, and, secondly, a molybdenum or tantalum ring, 0.170″ high with a 0.020″ wall thickness, was placed in direct contact with the graphite capsule and graphite furnace such that the central horizontal sections of the furnace and the ring coincide (Fig. 1). It was expected that the decrease in the resistance of the furnace owing to contact with the metal ring would flatten the temperature maximum at the furnace hot spot.

Kushiro (op. cit.) designed a graphite furnace with a 3° internal taper which was found to be very effective in flattening the temperature maximum. Our furnace design is simpler to fabricate than Kushiro's and its effectiveness was confirmed by a "dummy" experiment without the garnet sample, but in an otherwise similar pressure-cell as in the diffusion-couple experiments, with two thermocouple junctions 0.1 inch apart and symmetrically located with respect to the central section of the furnace. Temperature gradients, measured under constant pressure conditions, were found to be within 4° C at 1,300° C, with the interface position being hotter. Taking into account the temperature dependence of the temperature gradient near the hot spot of furnace (Cohen et al. 1967), we believe that the temperature of horizontal interface in our experiments up to 1,525° C was within 5° C of that sensed by the thermocouple. With respect to the vertical interface, we analyzed diffusion profiles from within 0.1″ from the thermocouple junction.

The metal ring, intended to smooth the temperature gradient, served the additional important purpose of protecting the couple-interface and thermocouple junction against the influx of molten glass or the CsCl insulating sleeve that almost invariably diked through the broken furnace at high temperature. The effectiveness of the ring in preventing the chemical attack of the garnet couple was revealed during dismemberment of the charge after run

completion. When talc-glass insulation was used, the molten glass would quite commonly dike through fractures in the furnace wall. Such ingress of glass was usually halted by the ring, and contamination problems were only apparent during very high temperature salt-cell runs. The fracturing of the furnace walls, which led to large power fluctuations, distortion of temperature distribution, and ingress of glass or salt causing partial melting of the garnet sample at high temperature, was greatly reduced by making the furnace slightly shorter (0.080 inch) than the insulating sleeve. The latter was prevented from collapsing radially underneath the furnace by a supporting steel ring. This design was suggested by Boettcher et al. (1981).

We developed the CsCl pressure cell during the course of this study in our effort to minimize fracturing of the carbide cores due to thermal stress in long runs at high $P-T$ conditions. CsCl proved to be a much superior insulating material to talc-glass or any other salt, except KBrII, which has been used before in high pressure cells. CsCl and KBrII, which has a CsCl structure, seem to have similar thermal conductivities, but KBrII is very difficult to use owing to (1) the fairly large volume change of the KBrI (NaCl structure) = KBrII transition around 17 Kbar (Pistorius 1965) that produces considerable distortion of the furnace, and (2) substantial melting near the furnace hot spot at conditions of our high temperature runs. However, for reasons that we do not completely understand, the garnet couple often partly melted during the high temperature runs with CsCl insulation, although the run condition was about 100° below the CsCl melting temperature, presumably due to leaching of Cs and/or Cl through the graphite furnace. Consequently, we continued to make runs with the classical talc-glass insulation, as the situation demanded, to minimize loss of the couple interface. The complete encapsulation of the sample, as shown in Fig. 1d, seemed to be effective in stopping the melting of garnet. The use of CsCl demonstrated some important points about the stability of the thermocouple and pressure cell, which are discussed below.

Pressure and temperature measurement

The nominal pressures, measured on a 16 inch diameter Heise gauge, were corrected on the basis of previous calibration experiments in similar pressure cells (e.g. Ganguly and Kennedy 1973; Mirwald et al. 1975). The determination of the sample temperature, which was measured by the relatively more stable W-3Re/W-25Re thermocouples, was, however, complicated by the possibility of progressive thermocouple decalibration at high temperature, especially in runs of long duration (Presnall et al. 1973). If the thermal and mechanical properties of the furnace-pressure cell assembly remain essentially the same during a run, then the power input to the furnace for a fixed sample temperature should remain stable after the first few hours required for the attainment of a stable thermal condition in the high pressure apparatus. Thus, we assumed a progressive change of the power drawn by the furnace to be indicative of thermocouple decalibration. Consequently, we switched to a power control mode, which controlled the furnace power within ± 2 watts, whenever the power continued to drift in the same direction for a long time. Such drift was invariably the case in runs with the talc-glass cell. However, the power was found to remain sufficiently stable in some of the subsequent experiments with the CsCl cell, especially if the nominal pressure was maintained constant, suggesting no significant thermocouple decalibration in runs at least up to 1,425° C. Since the internal parts of the graphite furnace were the same in all runs, especially around the thermocouple junction, we believe that the power variations in the other runs of similar duration were *not* due to the decalibration of the thermocouple. Instead, these were the results of the movement of furnace hot spot and variation of heat dissipation due to such factors as partial melting of the insulation, especially of glass, change in the rate of flow of cooling water, etc. Consequently, we calculated sample temperatures of *all* runs on the basis of thermocouple voltage. This midcourse modification of procedure resulted in an uncertainty of as much as $\pm 45°$ C in the temperature estimate for some very high temperature runs made under controlled power condition.

As there are no direct experimental data on the pressure effect on the emf of W/Re thermocouples, the nominal mean temperatures were corrected on the basis of Williams and Kennedy's (1969) data on the relative pressure effect on the emf of W/Re and Pt/Rh thermocouples, and Getting and Kennedy's (1970) data on the pressure effect on the latter. The corrected temperatures were 9 to 11° C higher than the nominal temperatures.

Diffusion profiles: measurement and results

The experimental diffusion profiles were measured using a 4-spectrometer ARL microprobe. The electron beam current and accelerating voltage were, in most cases, 50 na and 15 KV, respectively. The garnets were initially probed for homogeneity. A complete spot analysis was collected on one side of the couple away from the interface, then Fe, Mn, Ca and Mg counting rates were recorded simultaneously at 0.5 μm steps across the diffused region, where another full analysis was made. The two spot analyses bracketed the compositional range of the profiles. The two analyses were used to calculate a proportionality coefficient between counting rate and cation fraction as a function of counting rate by linear interpolation between the values of the spot analyses. The proportionality coefficient for each element for the counting rate at each point was calculated and used to reduce the data to cation fractions. This method yielded acceptably stoichiometric analyses across the diffusion profile. The technique minimizes potential drift problems, and distributes errors according to molar abundance (Loomis 1978). The complete spot analysis was reduced by the Bence-Albee method (Bence and Albee 1968). Multiple step-scanning traverses were made across each couple interface.

The spatial resolution of the microprobe spot analysis has been tested by analyzing across the interface of a garnet-garnet couple, and a garnet-aluminium metal couple, across which essentially no diffusion has occurred. The garnet-garnet couple was prepared by welding together the polished interface of a spessartine-almandine couple at 30 Kbar for 2.5 h at 1,200° C, followed by 9.5 h at 800° C. On the basis of our diffusion data, to be discussed later, the expected diffusion path length under these conditions is ~ 0.1 μm. The garnet-aluminium couple was prepared by inserting a piece of garnet into molten aluminium and quenching it immediately. The results of step scanning at a 0.5 μm interval at 15 KV, 50 na across the interfaces of

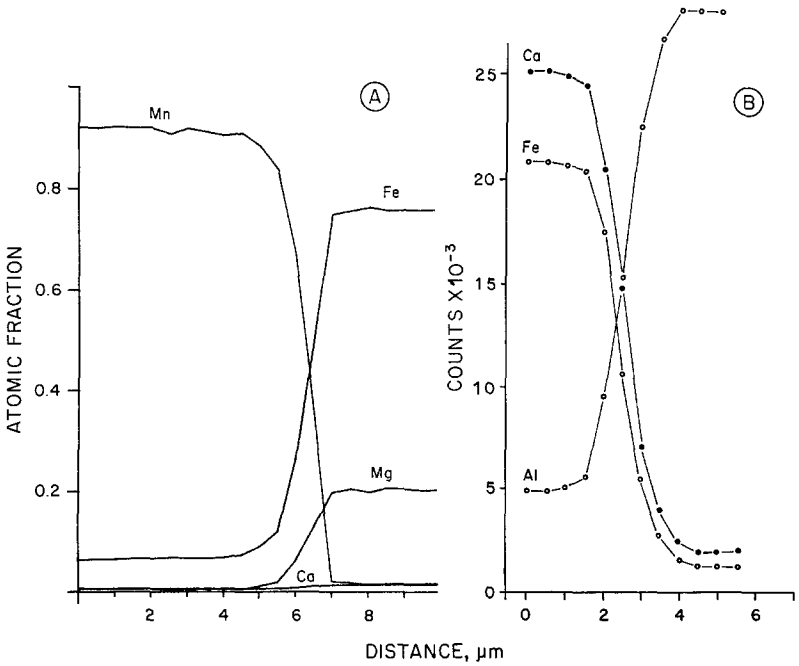

Fig. 3A, B. Illustration of the spatial averaging or convolution effect in microprobe analysis: **A** a spessartine-almandine couple subjected to 30 Kbar, 1,200° C, 2.5 hrs and 800° C, 9.5 h, and **B** an almandine-aluminium couple made by inserting a piece of almandine in molten aluminium and quenching immediately. Expected diffusive length in (a) is less than 0.1 μm. The analysis represent step-scanning at 0.5 μm intervals at 15 KV, 50 na accelerating voltage and beam current, respectively

these couples are illustrated in Fig. 3. The discontinuities at the interface are found to be smoothed, due to the spatial averaging, over ~3 μm in both cases. This smoothing, commonly known as the "edge effect", causes measured compositional gradients to be less than true and diffusion coefficients interpreted from the data to be larger than true. Step scanning using 10 and 20 na beam currents at both 15 and 10 KV accelerating voltages did not materially improve the resolution. Assuming that the excited x-ray intensity has a Gaussian spatial distribution, it can be estimated from the data in Fig. 3 that the Gaussian has a standard error of ~0.6 μm. The details of this analysis will be presented in a separate paper (Bhattacharya, Ganguly and Loomis, in preparation). Thus, ~66% of the excited X-rays have come from a volume with a horizontal cross-sectional radius of 0.6 μm concentric with the center of the incident electron beam.

The length of the experimentally induced diffusion profiles varied from 7 to 16 μm for pyrope-almandine couples and 20 to 30 μm for spessartine-almandine couples, depending on the experimental conditions, which are summarized in Table 1. Many profiles were found to have a narrow zone around the initial couple interface in which the compositional gradients were less steep than on either side. These anomalous zones were due to fine scale fracturing, and ranged from less than 1 μm to (an unacceptable) several μm. Thus, multiple step-scanning across an interface, and, in some cases, more than one experiment at the same condition were required before at least one profile could be found in which the effect of interfacial fracturing might be considered to be insignificant. Two examples of acceptable profiles are illustrated in Fig. 4. Figure 5 illustrates an unacceptable profile which has been extended by interfacial fracturing.

The measured profiles represent a combination of the true diffusion profiles and the spatial averaging of composition around the center of the electron beam. The latter effect would be most pronounced in the section of the profile showing the largest curvature, that is, at the terminal segments of the diffused zones, and, thus, will have the effect of enhancing the profiles. Obviously, the shorter profiles are subject to larger relative convolution. A mathematical formulation has been developed (Bhattacharya et al., op. cit.) to retrieve the true diffusion profile through deconvolution of the spatial averaging effect, and work is underway to refine and computerize the method. We have, however, ignored the convolution effect in our analysis of the experimental data in this and in the following paper, and have, therefore, selected only those profiles which are long enough (mostly larger than 15 μm) that the convolution effects would not be serious. These include all the data for the spessartine-almandine couple experiments, but exclude all but one pyrope-almandine profile. The rest of the pyrope-almandine data will be treated in a separate paper taking into account the convolution due to the spatial averaging of composition. We have chosen to include data for one pyrope-almandine couple here as these demonstrate some interesting compositional effects when considered along with the data for almandine-spessartine, as discussed in the following paper.

Interdiffusion of cations

The experimentally induced diffusion profiles clearly show that the interdiffusion of cations in both spessartine-almandine and pyrope-almandine couples depends on composition. This is illustrated in Figs. 6 and 7, in which the profiles in Fig. 4 are compared with those calculated using a *constant* interdiffusion coefficent D. The simulated profiles in

Table 1. Selected data for diffusion couple experiments

Run No.	Diffusion couple[a]	*P*, Kbar (±1 Kbar)	*T* (°C)	Time, (h)	Approximate diffused zone (μm)	$D(10^{13})$ cm²/s[c]		
						Fe-rich		Mg/Mn-rich
11	Pyr(1)-Alm(1)	40	1,340±10	72.75	7			
15	Pyr(1)-Alm(1)	40	1,370±40	76.33	9			
17	Pyr(2)-Alm(1)	40	1,440±30	94.80	10	1.09	(T7)[b]	0.10
						1.09	(T9)	0.20
16	Pyr(1)-Alm(1)	38	1,475±45	26.66	16			
40	Spess-Alm(2)	38	1,300±10	122	23	2.9	(T3)	1.4
						3.1	(T4)	1.5
43	Spess-Alm(2)	29	1,300±10	91	21	3.8	(T1)	2.4
						3.2	(T3)	1.8
						4.0	(T4)	2.5
31	Spess-Alm(2)	41	1,365±15	72	23	–	(T1)	3.7
38	Spess-Alm(2)	43.3	1,350±10	91	23	4.0	(T4)	1.5
29	Spess-Alm(2)	41	1,430±10	46.7	30	15.0	(T1A)	7.0
32	Spess-Alm(2)	41	1,480±15	36.6		15.0	(T2)	6.0
41	Spess-Alm(2)	41	1,475±10	25.0	24	15.0	(T1)	12.0
						14.0	(T5)	7.0

[a] Average Compositions:
Pyrope(1): $(Fe_{1.42}Mg_{1.45}Ca_{0.14}Mn_{0.03})Al_{2.05}Si_{2.93}O_{12}$
Pyrope(2): $(Fe_{0.48}Mg_{2.27}Ca_{0.24}Mn_{0.01})Al_{1.92}Si_{2.98}O_{12}$
Alm(1): $(Fe_{2.05}Mg_{0.85}Ca_{0.07}Mn_{0.02})Al_{2.02}Si_{2.99}O_{12}$
Alm(2): $(Fe_{2.42}Mg_{0.59}Ca_{0.03})Al_{1.97}Si_{3.02}O_{12}$
Spess: $(Fe_{0.17}Mn_{2.87})Al_{1.94}Si_{3.01}O_{12}$
[b] Microprobe traverse number
[c] See text for discussion of reproducibility of *D*

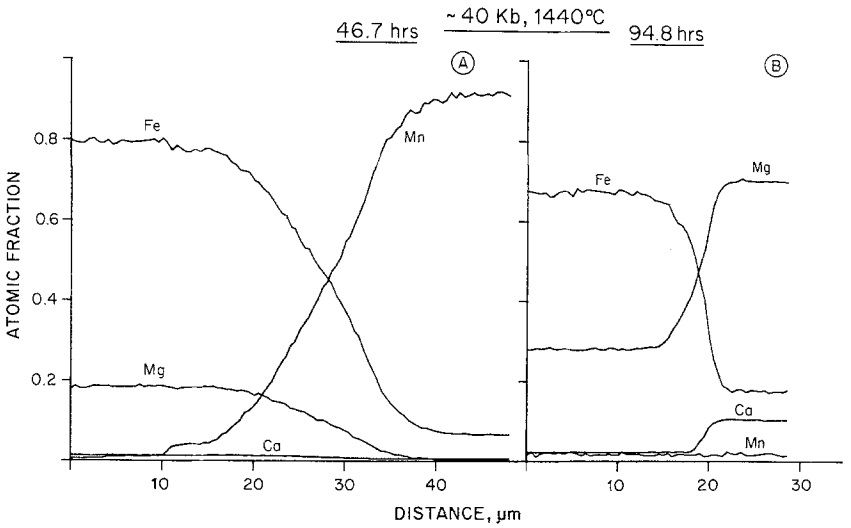

Fig. 4A, B. Illustration of experimentally induced diffusion profiles in **A** a spessartine-almandine couple (run # 29T1A) and **B** a pyrope-almandine couple (run # 17T9), which are acceptable for the purpose of retrieval of diffusion data. The experiments were at 40 Kbar, 1,440° C, for 46.7 and 94.8 h respectively. Notice that the spessartine-almandine profiles are longer than the pyrope-almandine ones in spite of shorter run duration.

these figures were computed by the analytical solution for diffusion with extended initial distribution of the diffusing species satisfying the initial boundary condition $C=C_0$ at $X<0$, $C=0$ at $X\geq 0$, $t=0$ (C=concentration, X=distance, t=time). For constant D, the solution to this diffusion problem is given by Crank (1975):

$$C(X,t)=1/2\,C_0\,\mathrm{erfc}(X/2(Dt)^{1/2}). \quad (1)$$

For the spessartine-almandine couple in Fig. 6 (Run # 29T1A), the experimental profiles required a variation of the interdiffusion coefficient D from 15×10^{-13} cm²/s for the Fe-rich side of the profile to 7×10^{-13} cm²/s for the Mn-rich side, whereas for the pyrope-almandine couple in Fig. 7 (Run # 17T9), D varied by nearly an order of magnitude, between 1.09×10^{-13} (Fe-rich side) and 0.20×10^{-13} (Mg-rich side) cm²/s.

The D values required to fit Fe- and Mn/Mg-rich compositions in each set of experimental profiles in a particular microprobe traverse are summarized in Table 1. Independent and multiple fittings of selected profiles suggest that the interdiffusion coefficients for the Fe- and Mn/Mg-rich compositions should be precise to within 20% of the tabu-

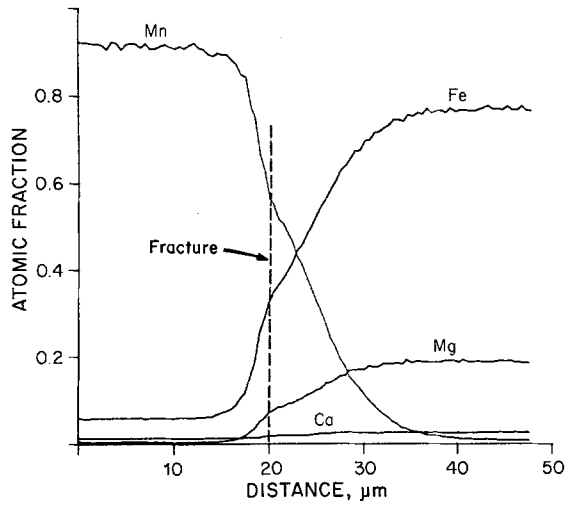

Fig. 5. An example of an "unacceptable" experimentally-induced diffusion profile in a spessartine-almandine couple in which the profile was extended by fracturing at the interface (Run # 31T3)

lated values. The interdiffusion data for the spessartine-almandine couple have been cast into the form of the Arrhenius equation,

$$D = D_0 \exp(-Q/RT), \tag{2}$$

where Q is the so-called activation energy (enthalpy) of diffusion, and D_0 is a constant related to the entropy of activation. The $\log_{10} D$ values are plotted against reciprocal temperature in Fig. 8. Linear least-squared fit of these data, ignoring the subjective estimates of errors in D and T, yielded $D_0 = 0.82 \times 10^{-5}$ cm^2/s, $Q = 53.6 \pm 4.9$ Kcal and $D_0 = 1.2 \times 10^{-5}$ cm^2/s, $Q = 57.1 \pm 8.4$ Kcal at 40 Kbar for interdiffusion in Fe-rich and Mn-rich compositions, respectively, in the spessartine-almandine couple. The D for the pyrope-almandine couple at 1,425° C, 40 Kbar is an order of magnitude slower than that in the spessartine-almandine couple at the same condition. (Our preliminary analysis (Elphick et al. 1981) of the Fe-Mg profiles, without regard to the convolution effects, suggested a much larger Q for Fe-Mg interdiffusion, in excess of 80 Kcal at 40 Kbar.)

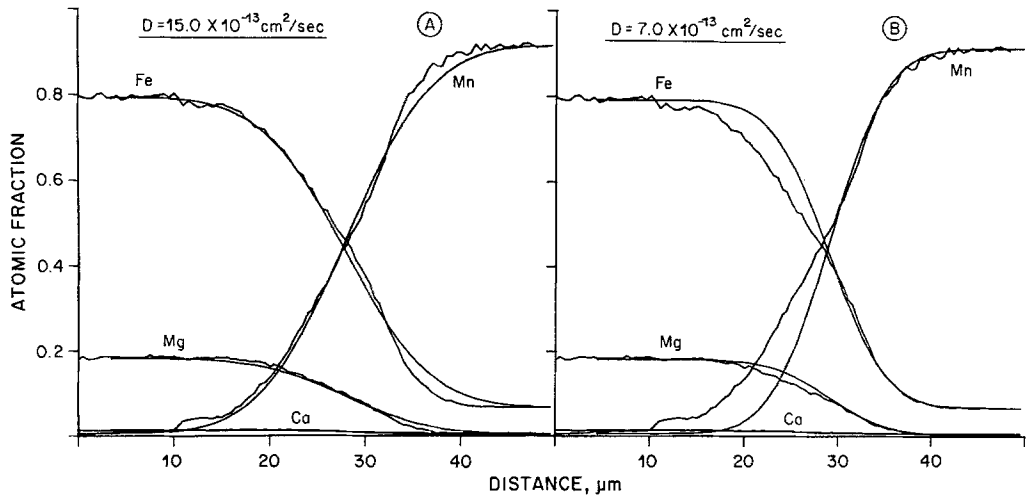

Fig. 6. Comparison of the spessartine-almandine diffusion profiles shown in Fig. 4(A) with those generated on the basis of constant interdiffusion coefficients (D). The profiles cannot be fitted by a constant D. The extreme fits (A: *left side;* B: *right side*) illustrate the approximate range of variation of D as a function of composition in the compositional range of this couple at ~40 Kbar, 1,440° C

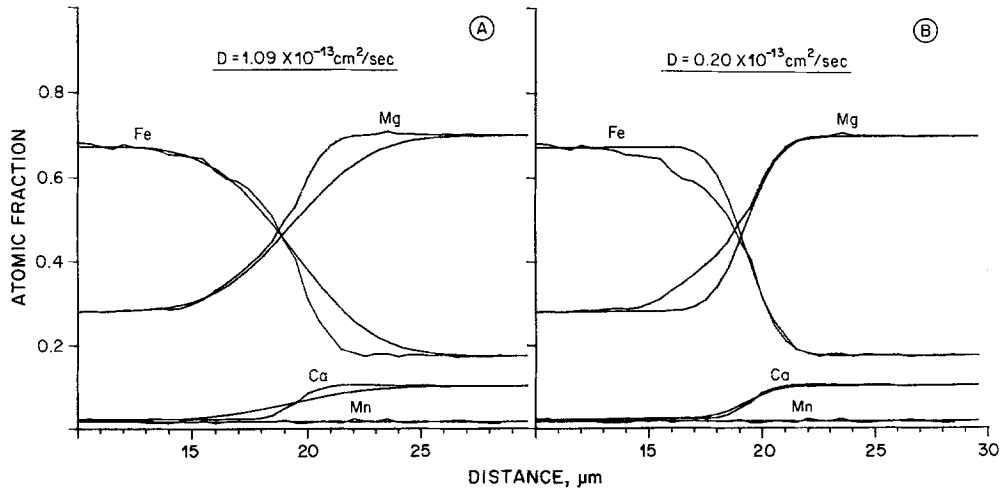

Fig. 7. Comparison of the pyrope-almandine diffusion profiles shown in Fig. 4(B) with those generated on the basis of constant D. See caption of Fig. 6

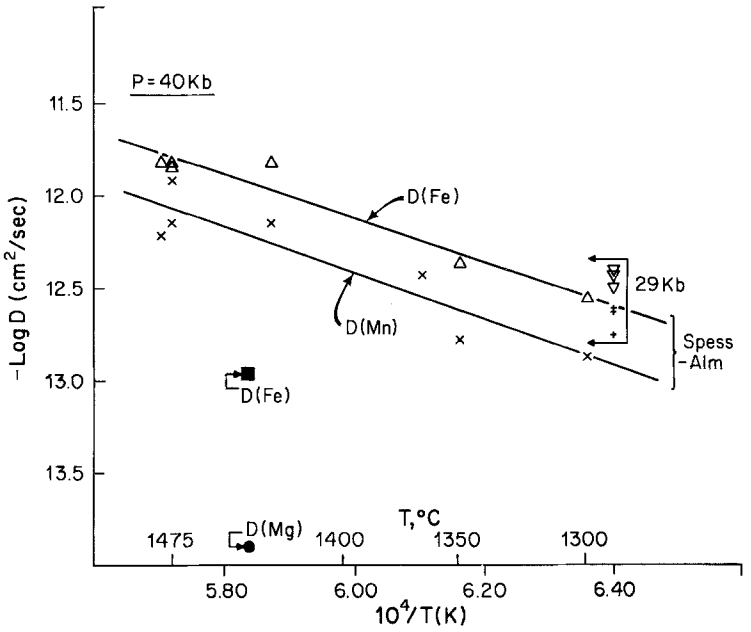

Fig. 8. Arrhenius plots of interdiffusion coefficients normalized to 40 Kb for spessartine-almandine couples: triangle: Fe-rich compositions; *X*: Mn-rich compositions. Values of *D* at 29 Kbar (Run # 3) are shown for comparison as: inverted triangle: Fe-rich compositions; cross: Mn-rich compositions. Data for Fe- and Mg-rich compositions in a pyrope-almandine couple (Run # 17T9) at 40 Kbar, 1,440° C are also shown for comparison

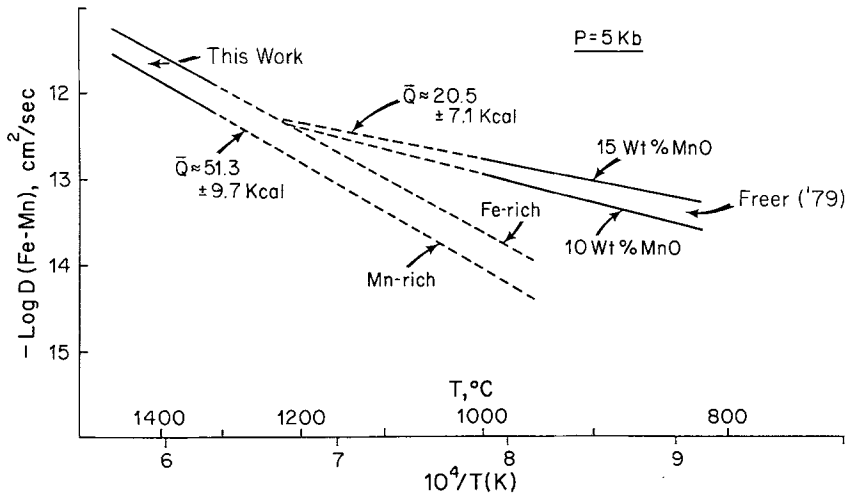

Fig. 9. Comparison of Fe-Mn interdiffusion coefficients determined in this work at 1,300–1,475° C with that determined by Freer (1979) at 800–1,002° C, both normalized to 5 Kbar. The experimental temperature ranges are shown by solid lines

In both spessartine-almandine and pyrope-almandine couples, the interdiffusion coefficent increases with increasing Fe^{2+}. A similar effect of Fe^{2+} on *D* has been documented for (Fe-Mg)-olivine (Misener 1974; Buening and Buseck 1973) and interpreted as due to (1) the increased equilibrium concentration of cation vacancies and Fe^{3+} owing to the increase of Fe^{2+} at constant oxygen fugacity, and (2) the expansion of the crystal lattice (Buening and Buseck 1973; Morioka 1980; Lasaga 1981). The Fe^{2+}-Mg order-disorder kinetics in orthopyroxenes, which is a diffusion controlled process, is also found to be enhanced by increasing Fe^{2+} concentration (Ganguly 1982). In contrast to our data on Fe-Mn interdiffusion, however, Freer (1979) has noticed an increase of *D* with *decreasing* Fe content in diffusion experiments using a sinter of $Mn_3Al_2Si_3O_{12}$ powder and almandine-rich garnet $(Mg_{0.93}Fe^{2+}_{2.07})Al_2Si_3O_{12}$ at 1 bar, 915–1,002° C.

The pressure dependence of the diffusion coefficient is given by the following relation

$$\left(\frac{\delta \log D}{\delta P}\right)_T = -\frac{\Delta V^+}{RT} \tag{3}$$

where ΔV^+ is the activation volume. We do not have adequate data to calculate ΔV^+, but an approximate value could be extracted by comparing the data for the Fe-Mn couple at 38 and 29 Kbar at 1,300° C. These data yield $\Delta V^+ = 4.7$ cm^3/mole, which may be compared with a value of 5.50 cm^3/mole for Fe-Mg interdiffusion in olivine (Misener 1974). Using this value, we obtain from (2) and (3)

$$\log D(P,T) = \log D_0(P^*) - \frac{Q(P)}{4.576\,T}, \tag{4}$$

where $Q(P) = Q(P^*) + 0.114(P - P^*)$ with *P* in atmospheres and *Q* in calories. We have, accordingly, extrapolated both our data and Freer's data on Fe-Mn interdiffusion to 5 Kbar, which is a geologically reasonable pressure for Fe-Mn garnets. The results are compared in Fig. 9. Our high temperature (1,300–1,475° C) data yield a much higher activation energy (51.3 ± 9.7 Kcal) than that required by Freer's data (20.5 ± 7.1 Kcal) in the temperature range 822 to 1,002° C. This difference could be due to a change of diffusion at 1,265° C from a high temperature "intrinsic" mechanism to a low temperature "extrinsic" mechanism (see, for example, Lasaga 1981). A similar change was noticed

in Fe-Mg and Co-Mg interdiffusions in olivine at 1,125 and 1,300° C respectively (Buening and Buseck 1973; Morioka 1980), although Misener's data do not suggest any abrupt change of D(Fe-Mg) in olivine. A change of diffusion mechanism in garnet is not, however, supported by the analysis of tracer diffusion data presented in Part II.

The validity of the Fe-Mn interdiffusion data can be tested by considering the time scale of homogenization of a zoned garnet crystal under medium grade metamorphic conditions. An approximate estimate of this time scale can be obtained from the solution of non-steady state diffusion in a sphere with fixed boundary concentration. When the composition at the center of a spherical grain of radius a has evolved through 95% of the original difference between the central and edge compositions, we have, from Crank (1975, eqn. 6.21), $Dt/a^2 \cong 0.4$. Thus, a spherical grain of garnet of 0.5 mm radius would essentially homogenize at 500–550° C within a time period of the order of 10^4 and 10^8 yrs according to Freer's and our diffusion data, respectively. The former estimate is incompatible with the common preservation of strong compositional (Fe-Mn) zoning in garnets of comparable dimension (and composition as used by Freer) in middle grade metamorphic rocks (e.g. Hollister 1969; Loomis 1983), and the 'reasonable' estimates of the cooling rate of $10–10^2$ °C/my for metamorphic rocks (Ganguly 1982; Lasaga 1983).

Duckworth and Freer (quoted in Freer 1981) have determined the Fe-Mg interdiffusion coefficient between 1,423 and 1,603° C at 30 Kbar. Their value for D(Fe-Mg), 6.11 $\exp(-41376/T)$ cm^2/s, yields a value for log D of -9.84 cm^2/s at 1,440° C, compared to the value -13.1 cm^2/s derived in this study for the same conditions (Table 1).

Acknowledgements. Research support on this project was provided by the Earth Sciences Section, National Science Foundation grant EAR79-19732. Thanks are due to Dr. Randall Cygan and an anonymous reviewer for their constructive reviews, and to Dr. Bernard Evans for assuming the editorial responsibilities and making suggestions for improvement.

References

Bence AE, Albee AL (1968) Empirical correction factor for the electron micro-analysis of silicates and oxides. J Geol 76:382–403

Boettcher AL, Windom KE, Bohlen SR, Luth RW (1981) Low-friction, anhydrous, low- to high-temperature furnace assembly for piston-cylinder apparatus. Rev Sci Instrum 52:1903–1904

Buening DK, Buseck PR (1973) Fe-Mg lattice diffusion in olivine. J Geophys Res 78:6852–6862

Cohen LH, Ito K, Kennedy GC (1967) Melting and phase relations in an anhydrous basalt to 40 kilobars. Am J Sci 265:475–518

Crank J (1975) The Mathematics of Diffusion (2nd ed). Clarendon Press, Oxford

Elphick SC, Ganguly J, Loomis TP (1981) Experimental study of Fe-Mg interdiffusion in aluminosilicate garnet. EOS (abstract), Tran Am Geophys Union 62:411

Freer R (1979) An experimental measurement of cation diffusion in almandine garnet. Nature 280:220–222

Freer R (1981) Diffusion in silicate minerals and glasses: a data digest and guide to literature. Contrib Mineral Petrol 76:440–454

Ganguly J (1982) Mg-Fe order-disorder in ferromagnesian silicates. In: Saxena SK (ed) II. Thermodynamics, kinetics, and geological applications, Springer. Adv Phys Geochem 2:58–99

Ganguly J, Kennedy GC (1973) The melting temperature of uranium at high pressures. J Phys Chem Solids 34:2272–2274

Getting IC, Kennedy GC (1970) Effect of pressure on the e.m.f. of chromel-alumel and platinum-platinum 10% rhodium thermocouples. J Appl Phys 41:4552–4562

Hollister LS (1969) Contact metamorphism in Kwoiek area of British Columbia: An end member of the metamorphic process. Geol Soc Am Bull 80:2456–2493

Kushiro I (1975) A new furnace assembly with a small temperature gradient in solid media, high-pressure apparatus. Carnegie Inst Washington Yearb 75:833–835

Lasaga AC (1981) The atomistic basis of kinetics. In: Lasaga AC, Kirkpatrick RJ (eds) Kinetics of Geochemical Processes. Rev Mineralogy 8:261–320

Lasaga AC (1983) Geospeedometry In: Saxena SK (ed) An extension of geothermometry, Springer. Adv Phys Geochem 3:81–114

Loomis TP (1978) Multicomponent diffusion in garnet: II. Comparison of models with natural data. Am J Sci 278:1119–1137

Loomis TP (1983) Compositional zoning of crystals. In: Saxena SK (ed) A record of growth and reaction history. Adv Phys Geochem 3:1–60

Loomis TP, Ganguly J, Elphick S (1985) Experimental determination of cation diffusivities in aluminosilicate garnets: II. Multicomponent simulation and tracer diffusion coefficients. Contrib Mineral Petrol 90:45–51

Morioka M (1980) Cation diffusion in olivine – I. Cobalt and magnesium. Geochim Cosmochim Acta 44:759–762

Mirwald PW, Getting IC, Kennedy GC (1975) Low friction cell for piston- cylinder high pressure apparatus. J Geophys Res 80:1519–1525

Misener DJ (1974) Cationic diffusion in olivine to 1,400° C and 35 Kbar. In: Hoffman AW, Gileti BJ, Yoder HS Jr, Yund RA (eds) Geochemical Transport and Kinetics. Carnegie Inst Washington Publication 634:117–129

Perkins D III (1983) The stability of Mg-rich garnet in the system CaO-MgO-Al_2O_3-SiO_2 at 1,000–1,300° C and high pressure. Am Mineral 68:355–364

Pistorius CWFT (1965) Melting curves of potassium halides. J Phys Chem Solids 26:1543–1548

Presnall DC, Brenner NL, O'Donnell TH (1973) Drift of Pt/Pt10Rh and W3Re/W25Re thermocouples in single stage piston-cylinder apparatus. Am Mineral 58:771–777

Williams DW, Kennedy GC (1969) Melting curve of diopside to 50 Kilobars. J Geophys Res 74:4359–4366

Received July 18, 1984 / Accepted January 15, 1985